

WILEY-VCH



European Chemical  
Societies Publishing

# Take Advantage and Publish Open Access



By publishing your paper open access, you'll be making it immediately freely available to anyone everywhere in the world.

That's maximum access and visibility worldwide with the same rigor of peer review you would expect from any high-quality journal.

**Submit your paper today.**



[www.chemistry-europe.org](http://www.chemistry-europe.org)

# Immobilized Eosin Y for the Photocatalytic Oxidation of Tetrahydroisoquinolines in Flow

Fabian Herbrik,<sup>[a, b]</sup> Sergio Rossi,<sup>[a]</sup> Miguel Sanz,<sup>[b]</sup> Alessandra Puglisi,<sup>[a]</sup> and Maurizio Benaglia\*<sup>[a]</sup>

A new easy-to-synthesize solid supported Eosin Y and its application in the building of a catalytic continuous flow reactor is reported. The fluidic device was employed to perform tertiary amines in-flow photooxidations followed by a nucleophile addition, with overall productivity increased by one order

magnitude. When using the iminium-ions in situ generated or in a telescoped fashion, the resulting Mannich-products were isolated with high diastereoselectivity and up to 90% enantioselectivity, simply using air as terminal oxidant.

## Introduction

In his 2008 famed study David MacMillan turned the spotlight back on photochemistry – more specifically on photoredox catalysis,<sup>[1]</sup> where the photochemical process to generate reactive radical species is combined with chiral enamines emerging from a organocatalytic cycle. Since his initial studies, significant progress has been made, especially in replacing the expensive and toxic metal-based photocatalysts with more environmentally benign organic dyes.<sup>[2]</sup> Organic molecules can be tailor made to exhibit a large range of either highly oxidizing potentials or even highly reducing potentials.<sup>[3]</sup> As an inexpensive and versatile dye, Eosin Y exhibits intermediate oxidation and reduction potentials, and found numerous applications.<sup>[4]</sup>

Generally photochemistry suffers from poor scalability as the Lambert-Beer-Law dictates a negative exponential attenuation of photons through the reaction mixture. Most of the volume of a given batch reactor will not be efficiently irradiated. To overcome this limitation continuous flow reactors, due to their intrinsic higher surface-to-volume-ratio, are often used.<sup>[5–6]</sup> Notable examples of the combination of continuous technologies and Eosin Y are the pre-pilot water treatment reactor by Noel et al.,<sup>[7]</sup> or the luminescent solar concentrator reactor by Noel et al.<sup>[8]</sup>

In order to facilitate work-up and purification, also for economic reasons, the usage of solid supported (photo)-

catalysts is often preferred, best in small particulate forms to guarantee a high surface area. Eosin Y has been studied in this regards by supporting it as the counter-ion to ion-exchange resin,<sup>[9]</sup> on magnetic nanoparticles by ionic tethering,<sup>[10]</sup> graphene oxide,<sup>[11–12]</sup> backbone of metal organic frameworks,<sup>[13–14]</sup> backbone of porous conducting organic polymers.<sup>[15–16]</sup> In all cases work-up and purification were greatly facilitated

## Results and Discussion

With this study we wish to report an easy-to-synthesize solid supported Eosin Y and its application in the creation of a catalytic continuous flow reactor employed to perform tertiary amines oxidations followed by a nucleophile addition, to realize a diastereoselective Mannich type reaction.

As previously mentioned, the condensation of the strongly absorbing photocatalyst into small particulate forms represents a viable option to overcome the issue of the not efficient irradiation of the bulk of the reaction mixture. Therefore, we decided to investigate the use of an Eosin Y immobilized on the most commonly used precursor polymer for solid phase peptide synthesis – Merrifield-resin (as already reported in the literature)<sup>[17]</sup> It is itself a terpolymer of styrene, 4-vinylbenzylchlorid and 1–2% divinylbenzene as crosslinker. The resulting polymer beads from emulsion polymerization are macroscopic in size ( $\varnothing = 75 \mu\text{m}$ ) and become, when swollen, a free-flowing powder sufficiently soft to not grind down each other when agitated. The previously described strategies for solid supported Eosin Y)<sup>[18]</sup> explored either complicated bottom-up approaches for the synthesis of new materials or weak undirected interactions for the immobilization, such as ionic interactions (limiting scope and usability). In Scheme 1 a straightforward synthetic strategy for the immobilization of Eosin Y onto Merrifield-resin (High-loading 1.2 mmol/g) is displayed.

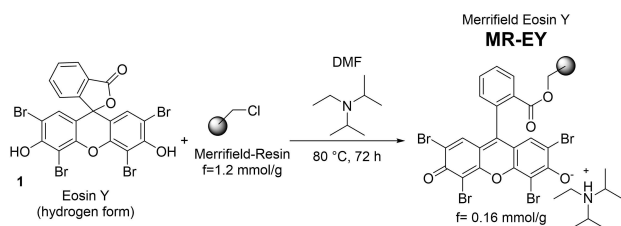
Eosin Y in its inactive hydrogen form is deprotonated and reacts as nucleophile with the Merrifield-resin (20 g scale). After three days the mixture is poured into a glass sintered funnel and extensively washed until the running liquids show no sign of pink color anymore. This covalent approach for the

[a] F. Herbrik, Dr. S. Rossi, Prof. A. Puglisi, Prof. M. Benaglia  
Dipartimento di Chimica  
Università degli Studi di Milano  
Via Camillo Golgi 19, 20133 Milano (Italy)  
E-mail: maurizio.benaglia@unimi.it

[b] F. Herbrik, Dr. M. Sanz  
Taros Chemicals GmbH & Co. KG  
Emil-Figge-Strasse 76 A, 44227 Dortmund, Germany

Supporting information for this article is available on the WWW under <https://doi.org/10.1002/cctc.202200461>

© 2022 The Authors. ChemCatChem published by Wiley-VCH GmbH. This is an open access article under the terms of the Creative Commons Attribution License, which permits use, distribution and reproduction in any medium, provided the original work is properly cited.



Scheme 1. Synthesis of solid supported Merrifield-resin Eosin Y (MR-EY).

preparation of solid supported catalyst should in principle give a more durable material.

The maintenance of the morphological integrity of the support was confirmed by SEM analysis on MR-EY (Figure 1). The EDS spectrum of MR-EY shows the peaks of Bromine atoms, that can be attributed to the anchoring of Eosin Y onto the polymer. The peaks of Chlorine atoms that are visible in the spectrum are ascribable to residual Cl atoms of the Merrifield resin that were not substituted by Eosin. As expected, the functionalization of the Merrifield resin is incomplete and this is also confirmed by the loading determined by both elemental analysis and weight difference, and the presence of Br in the new material (see Supporting Information for further details).

Next, the efficacy of the newly synthesized material was explored by using it in a well-established transformation, like the oxidation of a tertiary amine to the respective iminium-ion. Furthermore, following the supported-Eosin catalyzed oxidation step, a Mannich-type nucleophile addition to the in situ generated iminium ion was also investigated. Using 1,2,3,4-tetrahydroisoquinolines as amines, the iminium-ions can usually be isolated and even stored for prolonged periods of time due to the extensive  $\pi$ -conjugation, making them ideal substrates for this transformation.

As a starting point the CDHC was studied with the sodium salt of Eosin Y under homogeneous conditions (Scheme 2).

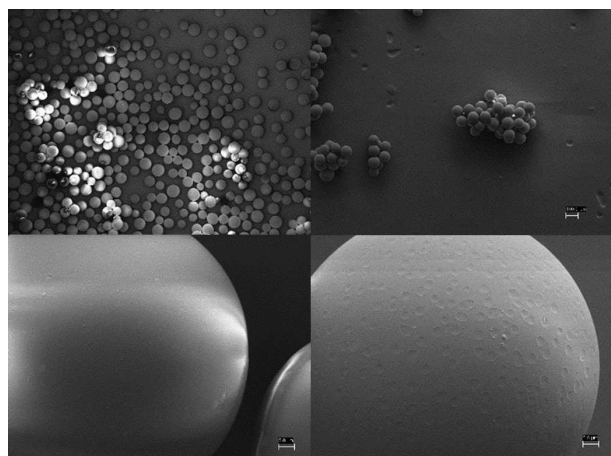
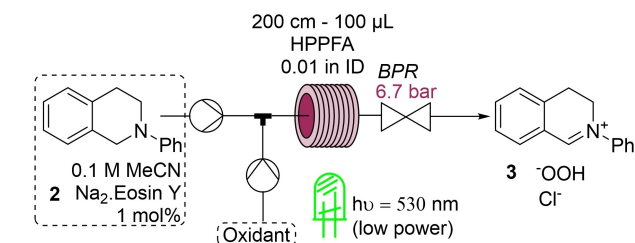
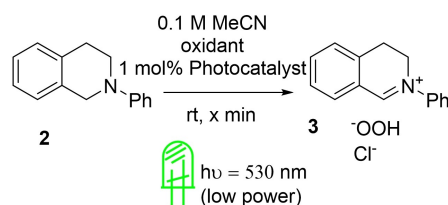


Figure 1. SEM images. a) Merrifield resin 150x magnification; b) MR-EY 150x magnification; c) Merrifield resin 4kx magnification; d) MR-EY 4kx magnification.

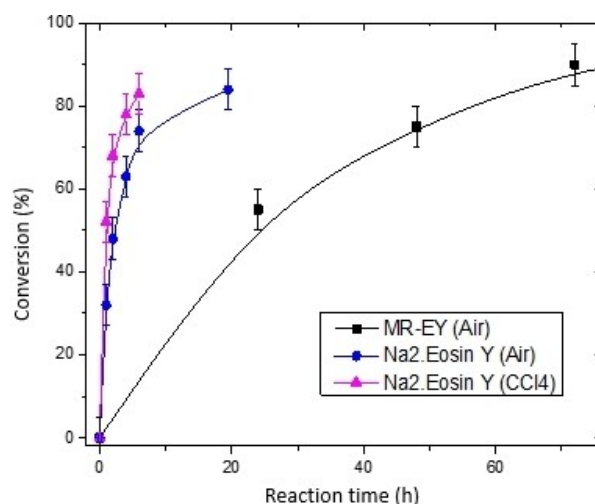


Scheme 2. Reaction conditions for batch and flow oxidation under homogeneous conditions.

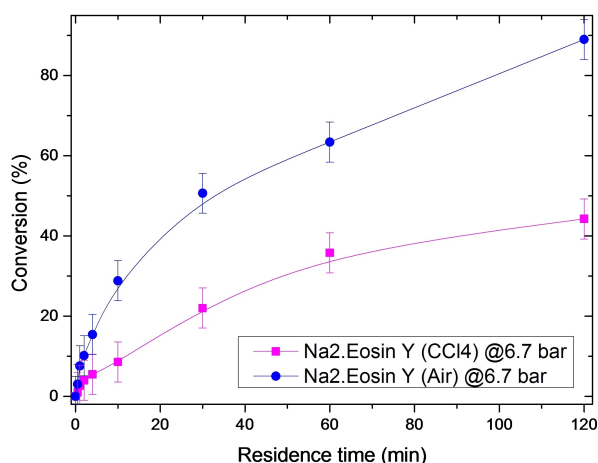
Typically, using either air or carbon tetrachloride as terminal oxidant, the reaction proceeds to good levels of conversion only in long times (10–20 h, Scheme 3). When MR-EY is employed, the reaction slows down by a factor of roughly 4. The combination of a triphasic reaction mixture (solid-liquid-gas) with an additional critical reaction parameter – light – that imposes another interfacial challenge is responsible for the observed lower reactivity, as mixing becomes more turnover limiting.

When Eosin Y is employed in a coiled microfluidic reactor setup, a significant speed up ( $\times 8$ ) is observed using air as oxidant and sevenfold increased pressure, leading to a 90% conversion after 120 min (Scheme 4).

The aforementioned additional interfacial challenges can be exploited when building a packed-bed catalytic continuous



Scheme 3. Conversion vs Reaction time graph of MR-EY and standard Eosin Y under batch conditions.

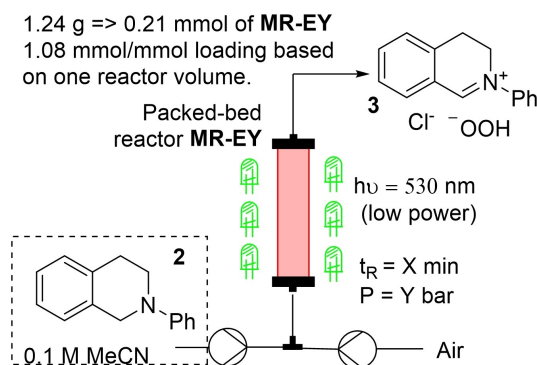


**Scheme 4.** Reaction Conditions for flow oxidation under homogeneous conditions.

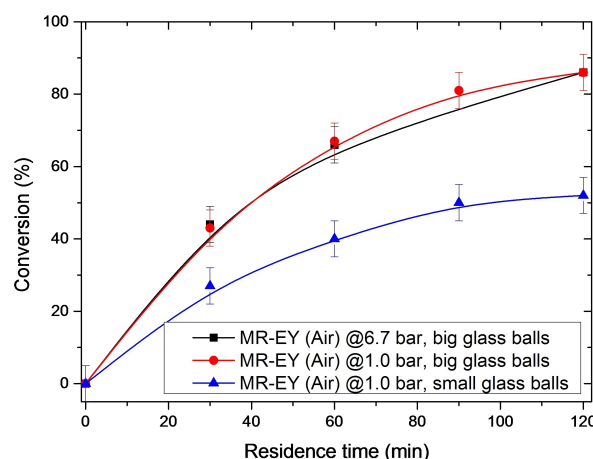
flow reactor. A 100×10 mm omnifit column was first maximally filled with 5 mm glass balls that were stacked in an alternating fashion and then MR-EY was filled inside as a suspension in acetonitrile.<sup>[18]</sup> This reactor design is aimed at increasing the internal irradiation of the reactor bulk and reducing the loading of the catalytic reactor. This reactor is then wrapped with low-power LED-strip (2.6 W/m) emitting at 530 nm (Scheme 5).

We were delighted to find out that the catalytic reactor performs roughly equal to the microfluidic reactor with homogeneous Eosin Y. After 120 min 86% of conversion was achieved, outcompeting the batch methodology by a factor of ~10×.

If 6.7 bar of air pressure was applied, no significant difference was observed. Only when reducing the size (and thus increasing the amount) of the glass balls inside the reactor, a significant difference in behavior was observed, cutting productivity in half and leading to a plateau-effect. These findings are summarized in Scheme 6. The difference in the amount of MR-EY inside the two catalytic reactors is not that significant enough to account for this different behavior. It is therefore



**Scheme 5.** Solid supported Eosin-promoted in-flow oxidation in a packed-bed reactor.



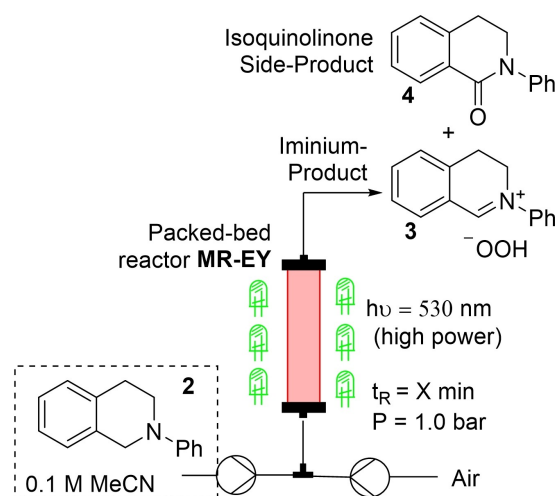
**Scheme 6.** Conversion vs residence time graph of solid supported Eosin Y in a packed bed reactor under continuous flow conditions.

hypothesized that the phenomenon should be ascribed to an irradiation effect.

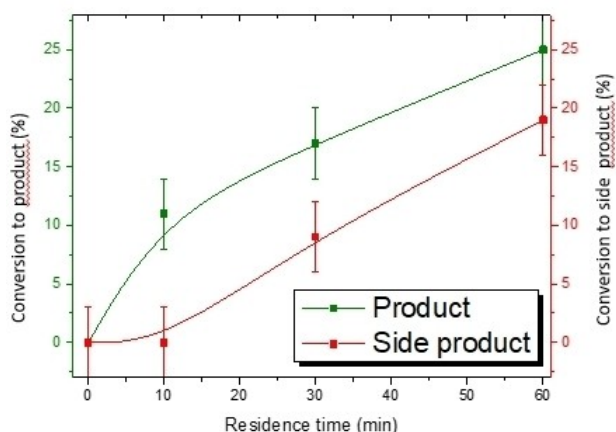
To further investigate the effect of photon density a high-power LED-strip (24 W/m) was employed next. Wrapping it around the catalytic reactor proved to be dangerous, as the LEDs would warm up the setup above the boiling point of acetonitrile. Even air-cooling did not cool down the catalytic reactor enough to reach room temperature, when 5 cm of distance between LEDs and reactor was guaranteed. A new device was thus built, by wrapping the LEDs around a double walled glass-piece that could be water-cooled (Scheme 7).

In Scheme 8 are summarized the findings with high power LEDs.

Unfortunately, to our surprise, the reaction did not speed up, but a significant amount of the isoquinolinone 4 side-product started to form, which was previously only hinted at in the HPLC-MS assay that was so far used to quantify. Assuming



**Scheme 7.** In-flow oxidation with high-intensity LED together with MR-EY packed-bed reactor.

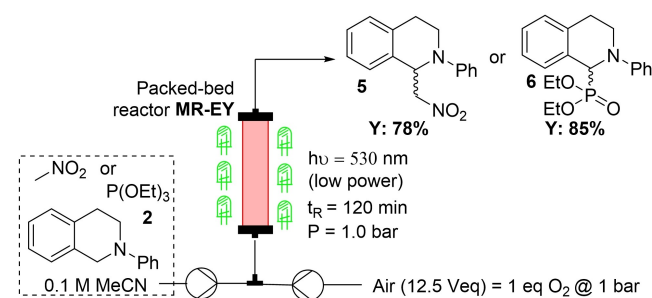


**Scheme 8.** Conversion (to the product and isoquinolinone side product respectively) vs residence time graph for the In-flow oxidation with high-intensity LED together with MR-EY packed-bed reactor.

an additional equivalent of oxygen is needed for the over-oxidation to the side-product, the conversion of product vs side-product (roughly 20%+20% respectively) indicates that from the 1.0 equivalents of oxygen that were infused into the reactor roughly 60% were consumed (at 1 h residence time), which is comparable to the consumption using low-power LED-strips (see Scheme 3).

Having found conditions with high productivity of iminium-ion generation, the in situ nucleophile addition was then undertaken. In preliminary investigations, nitromethane and triethylphosphite were selected as nucleophiles. Ten equivalents of  $\text{CH}_3\text{NO}_2$  or one equivalent of  $\text{P}(\text{OEt})_3$  were mixed with the tetrahydroquinoline **2** solution in acetonitrile before infusion into the catalytic reactor as displayed in Scheme 9. After 120 min of residence time and collection, the Aza-Henry-product **5** was isolated in 78% after chromatographic purification. Similarly, the phosphonate-product **6** was obtained in 85% isolated yield.

Next, a diastereoselective Mannich-protocol was translated into continuous flow. In a recently published visible-light-promoted, asymmetric cross-dehydrogenative coupling of tertiary amines to ketones, two different metal-based catalysts were necessary, one for the photooxidation, the other to reduce



**Scheme 9.** All-in-flow in situ addition of nucleophiles to generated iminium-ions.

nitrobenzoic acid to close the net oxidative process.<sup>[19]</sup> We decided to improve this protocol with our catalytic reactor by eliminating the metal catalysts and employing air as terminal oxidant.

Various chiral diamines were investigated as organocatalysts in the reaction of tetrahydroquinolines with cyclic ketones as Mannich donors. (see Table 1). We envisioned a two-step process as to avoid any potential side-reactions with the amino-catalyst inside the catalytic reactor. Yang et al found in their study that running the reaction under air condition would lead to subpar performance, probably due to catalyst decomposition.<sup>[19]</sup> Thus, the mixture containing the iminium-ion was combined only after photooxidation with the cyclic ketone and diamino catalyst and left to react in a semi-batch fashion in a temperature-controlled environment.

In Table 1 are summarized the findings after collection and chromatographic purification of the Mannich products, from the combination of cyclohexanone with differently substituted tetrahydroquinolines. Generally, when the reaction was performed at room temperature, low levels of diastereo- and enantioselectivity were obtained (entries 1–4). This protocol

**Table 1.** Diastereoselective Mannich reaction.

Entry	R	Catalyst	T [°C]	d.r.	e.e. [%]	Yield [%]
1	Ph	Cat-1 H <sub>2</sub> N-CH <sub>2</sub> -N(CH <sub>2</sub> ) <sub>2</sub> -CH <sub>2</sub> -N(CH <sub>2</sub> ) <sub>2</sub> -H	rt	60:40	–	64
2	Ph	Cat-2 H <sub>2</sub> N-CH <sub>2</sub> -N(CH <sub>2</sub> ) <sub>2</sub> -CH <sub>2</sub> -N(CH <sub>2</sub> ) <sub>2</sub> -H	rt	60:40	Rac (min) 2 (maj)	71
3	Ph	Cat-3 H <sub>2</sub> N-CH <sub>2</sub> -N(CH <sub>2</sub> ) <sub>2</sub> -CH <sub>2</sub> -N(CH <sub>2</sub> ) <sub>2</sub> -H	rt	55:45	67 (min) 70 (maj)	64
4	Ph	Cat-4 H <sub>2</sub> N-CH <sub>2</sub> -N(CH <sub>2</sub> ) <sub>2</sub> -CH <sub>2</sub> -N(CH <sub>2</sub> ) <sub>2</sub> -H	rt	15:85	33 (min) 45 (maj)	67
5	Ph	Cat-3 H <sub>2</sub> N-CH <sub>2</sub> -N(CH <sub>2</sub> ) <sub>2</sub> -CH <sub>2</sub> -N(CH <sub>2</sub> ) <sub>2</sub> -H	–10	83:17	88 (maj) 28 (min)	69
6	p-Cl-Ph	Cat-3 H <sub>2</sub> N-CH <sub>2</sub> -N(CH <sub>2</sub> ) <sub>2</sub> -CH <sub>2</sub> -N(CH <sub>2</sub> ) <sub>2</sub> -H	–10	80:20	90 (maj) 20 (min)	68
7	p-Br-Ph	Cat-3 H <sub>2</sub> N-CH <sub>2</sub> -N(CH <sub>2</sub> ) <sub>2</sub> -CH <sub>2</sub> -N(CH <sub>2</sub> ) <sub>2</sub> -H	–10	3.8:1	87 (maj) 5 (min)	61

was therefore modified and optimized using the most efficacious catalyst (cat 3) at room temperature (entry 3). At  $-10^{\circ}\text{C}$  after 3 days, the product was obtained in 69% yield and greatly improved diastereoselectivity (83:17), with very good enantioselectivity (88% e.e., entry 5).

Similar results were obtained also in the reaction with the *N*-*p*-bromo and *p*-chlorophenyl tetrahydroquinoline derivatives, where high diastereo- and enantioselectivity, up to 90% e.e., were observed (entries 6–7).

Finally, the recyclability of the supported photocatalyst was investigated. Under the employed reaction conditions, no significant deterioration of MR-EY was observed; for example, the same catalytic reactor has been employed to perform the initial screening experiments at 1.0 bar pressure (Scheme 3), when ten reactions, at five different residence time, were performed. The experiments were then duplicated, without observing any appreciable change in catalyst activity (see Tables 2 and 3 in the Supporting Information).

A single reactor was used also to run different stereoselective Mannich reactions, reported in Table 1. After every reaction, the reactor was extensively washed (> 20 reactor volumes), simply to make sure the out-flow running liquids contained no contaminants. After washing, different reaction conditions were applied, being the reactor itself always the same. The diastereoselective nucleophile additions (Table 1) were performed with the same reactor, that was reused for weeks in our study and did not have to be altered by any means.

## Conclusion

In conclusion, with the easy-to-synthesize new material MR-EY efficient photooxidation of tertiary amines was realized, especially operating with continuous flow catalytic reactors. Due to the greater mass transfer-efficiency of fluidic devices the overall productivity was increased by one order magnitude. When using the iminium-ions in situ or in a telescoped fashion the resulting Mannich-products could be isolated with high degrees of diastereoselectivity and enantioselectivity (up to 90% e.e.). Noteworthy, previous studies needed a metal-based photocatalyst for the initial photooxidation, in combination with another metal-based catalytic cycle with nitrobenzoic acid, to enable the same chemistry, that we accomplished simply using air as terminal oxidant. For this overall study the same reactor was reused several times, with no loss of efficiency and no apparent material degradation, indicating excellent stability and recyclability of the solid-supported on Merrifield-resin Eosin Y, MR-EY.

## Experimental section

### General Description of Reagents and Methods

As oxidation with air is one of the key scopes of this work, no special care was undertaken to work under an inert-gas atmos-

phere. If not otherwise stated reagents, solvents and such were used without further purifications. 1,2,3,4-tetrahydroisoquinoline was bought from sigma and distilled and stored over potassium hydroxide before use. Eosin Y was bought from TCI chemicals and was either used without purification or was converted to the sodium salt by addition aqueous sodium hydroxide solution. *N,N*-dimethylformamide was degassed prior to use. *N,N*-diisopropylethylamine was used without prior purification. Merrifield Resin High Loading 1.2 mmol/g was purchased from Merck. Acetonitrile was used in HPLC-grade quality. For analytical techniques see the SI.

### Experimental Procedures

#### Packed-Bed-reactor

100 mm × 10 mm (I\*ID) Omnifit-Column filled with:

Configuration 5 mm: A total of 42 5 mm glass-balls were filled inside the Omnifit-column (such that the glass-balls were forming a tight-packed configuration, 2 per layer) which was tightly held in place in a vertical position. Inside the column was filled a suspension of 1.24 g of Merrifield Eosin Y in acetonitrile. Regular agitation of the setup ensured complete settling of the solid material inside the reactor. After filling was completed the closing lid with fluidic connection was reattached. The reactor volume  $V_R = 1.95$  mL was determined by infusing a 0.1 M solution of anthraquinone and periodically (every 50  $\mu\text{L}$ ) collecting a drop of the outflow on a piece of TLC-plate and checking by a 254 UV-lamp.

#### Synthesis and Characterization of Solid-Supported Eosin Y MR-EY

In a 250 mL three-necked-flask were weighed exactly 10.0 g (8.33 mmol, 1.00 eq,  $f = 1.20$  mmol/g) Merrifield-Resin High-Load 100–200 mesh. To this were added 6.48 g (10.0 mmol, 1.20 eq) Eosin Y (hydrogen form). To the flask was then applied a mechanical stirring device. The solid were dispersed in 133 mL *N,N*-dimethylformamide. Mechanical stirring was turned on and it was added 3.48 mL (20.0 mmol, 2.40 eq) diisopropylethylamine. After setting the temperature to  $80^{\circ}\text{C}$  the dispersion was stirred for exactly 72 h.

After the reaction was completed the reaction mixture was poured into an oven-dried sintered glass funnel (pore size 4, pre-weighed) and special care was taken to remove almost all the material out of the flask with generous amounts of methanol. The residue was infused with a mixture of water/THF/methanol and stirred with a glass rod. After infusing for 5 minutes vacuum was attached and the washing liquid was filtered off. Vacuum was detached and the whole process was repeated 15 times. After this generous washing, the process was repeated for three times using dichloromethane. The washing flasks was changed and the remains in the funnel were dried by running a constant air stream through them for 5 hours by attaching a vacuum. After this time the filter was weighed again and by the difference in weight a preliminary catalyst loading calculated, which amounts to  $f = 0.168$  mmol/g.

Elemental analysis of MR-EY: C 80,73, H 6,54, N 0,28

That corresponds to  $f = 0.2$  mmol/g

The gravimetric loading ( $f = 0.168$  mmol/g) was used in the reactions.

### General Procedure for Plug-Flow Oxidation (Microfluidic Experiments (Screening))

Inside a screw-neck vial was prepared a 0.1 M solution of N-Phenyl 1,2,3,4-tetrahydroisoquinoline, 1 mM of Na<sub>2</sub>Eosin Y. In case of oxidation with tetrachlorocarbon the same solution was made with 0.15 M of tetrachlorocarbon. The solution was taken up in a 2.5 mL SGE gastight syringe and connected to the continuous-flow reactor.

Continuous flow reactor: 200 cm of HPFA HPLC-tubing was wrapped around a 2 cm diameter glass-tube. The resulting coil-reactor was connected via a Y-connector to the syringe (and the VapourTec peristaltic pump in case of aerobic oxidation), at the intake side. At the output side was connected a back-pressure-regulator (spring-loaded) ensuring 6.7 bar of pressure. The coil-reactor was placed inside the previously described batch-photo-reactor inside the crystallization dish as illustrated in the pictures in the Supporting Information.

The solution was infused inside the coil-reactor according to the tables and graphs in the Supporting Information. Between or before each collection at a previously varied flow rate, two residence times were discarded until steady state operation of the reactor was reached. Collection of an aliquot: 20  $\mu$ L, 2 drops were dissolved in 1.5 mL acetonitrile and injected into HPLC-MS for quantification.

### General Procedure for Continuous Flow Packed Reactor Oxidation Experiments (Screening)

Inside a screw-neck vial was prepared a 0.1 M solution of N-Phenyl 1,2,3,4-tetrahydroisoquinoline. The solution was taken up in a 25 mL SGE gastight syringe and connected to the continuous-flow reactor.

Continuous flow reactor: Either configuration (4 mm or 5 mm) was connected via a Y-connector to the syringe and the VapourTec peristaltic pump at the intake side. At the output side was connected a back-pressure-regulator (spring-loaded) ensuring 6.7 bar of pressure, in case of pressurized operation. The catalytic packed-bed reactor was wrapped with the low-power LEDs as previously specified. In case high power LEDs were employed the reactor was placed inside a doubled-walled reactor glass-piece which was connected to in-house water circulation/cooling system. Around this reactor was wrapped the high-power LED strip.

The solution was infused into the catalytic packed-bed reactor according to the tables and graphs in the Supporting Information. Between or before each collection at a previously varied flow rate, two residence times were discarded until steady state operation of the reactor was reached. Collection of an aliquot: 20  $\mu$ L, 2 drops were dissolved in 1.5 mL acetonitrile and injected into HPLC-MS for quantification.

### Fluidic Synthesis: General Procedure

Inside a screw-neck vial was prepared a 0.1 M solution of N-Phenyl 1,2,3,4-tetrahydroisoquinoline (or its para-chloro/para-bromo derivatives). The solution was taken up in a 25 mL SGE gastight syringe and connected to the continuous-flow reactor.

In case of Aza-Henry reaction (synthesis of product 5), nitromethane was added to generate a 1.0 M thereof.

In the synthesis of product 6, triethylphosphite was added to generate a 0.1 M solution thereof.

Continuous flow reactor: Configuration (4 mm or 5 mm) was connected via a Y-connector to the syringe and the VapourTec peristaltic pump at the intake side. At the output side was connected a back-pressure-regulator (spring-loaded) ensuring 6.7 bar of pressure, in case of pressurized operation. The catalytic packed-bed reactor was wrapped with the low-power LEDs as previously specified.

The solution was infused into the catalytic packed-bed reactor according to the tables and graphs in the Supporting Information. Between or before each collection at a previously varied flow rate, two residence times were discarded until steady state operation of the reactor was reached. Collection of an aliquot: 20  $\mu$ L, 2 drops were dissolved in 1.5 mL acetonitrile and injected into HPLC-MS for quantification.

After reaching satisfying levels of conversion the output of the packed-bed reactor was collected, or in the case of the diastereoselective Mannich-reaction protocol, connected to a Y-adapter into which was infused a solution of 15.0 M cyclohexanone and 1.0 M of the respective diamino-catalyst. The Y-adapter was inserted through a rubber-septum inside a temperature controlled (either room temperature or pre-cooled to  $-10^{\circ}\text{C}$ ) vial. The overall output was collected inside this vial and stirred for three days.

For further characterization and analytical data see the SI.

### Acknowledgements

A. P. thanks MUR for the project PRIN 2017 "SURSUMCAT". M. B. and F. H. thank ITN-EID project Marie Skłodowska-Curie Actions Innovative Training Network – TECHNORAIN H2020-MSCA-ITN-2018 Grant Agreement 812944. [www.technorain-ITN.eu](http://www.technorain-ITN.eu). M. B. and M. S. thank Taros Chemicals. Open Access funding provided by Università degli Studi di Milano within the CRUI-CARE Agreement.

### Conflict of Interest

The authors declare no conflict of interest.

### Data Availability Statement

The data that support the findings of this study are available from the corresponding author upon reasonable request.

**Keywords:** catalytic reactor · enantioselective catalysis · flow chemistry · photooxidation · supported catalyst

- [1] D. A. Nicewicz, D. W. C. MacMillan, *Science* **2008**, *322*, 77–80.
- [2] S. G. E. Amos, M. Garreau, L. Buzzetti, J. Waser, *Beilstein J. Org. Chem.* **2020**, *16*, 1163–1187.
- [3] E. Speckmeier, T. G. Fischer, K. Zeitler *J. Am. Chem. Soc.* **2018**, *140*, 15353–15365.
- [4] a) V. Srivastava, P. P. Singh, *RSC Adv.* **2017**, *7*, 31377–31392; b) F. Herbrink, P. Camarero González, M. Krstic, A. Puglisi, M. Benaglia, M. Sanz, S. Rossi, *Appl. Sci.* **2020**, *10*, 5596–5611.
- [5] Recent reviews: a) L. Buglioni, F. Raymenants, A. Slattery, S. D. A. Zondag, T. Noël, *Chem. Rev.* **2022**, *122*, 2752–2906; b) L. Marzo, S. K.

- Pagire, O. Reiser, B. König, *Angew. Chem. Int. Ed.* **2018**, *57*, 10034–10072; *Angew. Chem.* **2018**, *130*, 10188–10228; c) F. Strieth-Kalthoff, M. J. James, M. Teders, L. Pitzer, F. Glorius, *Chem. Soc. Rev.* **2018**, *47*, 7190–7202; d) M. Silvi, P. Melchiorre, *Nature* **2018**, *554*, 41–49.
- [6] Review on enantioselective photocatalysis: C. Prentice, J. Morrisson, A. D. Smith, E. Zysman-Colman, *Beilstein J. Org. Chem.* **2020**, *16*, 2363–2441.
- [7] D. Cambié, C. Bottecchia, N. J. W. Straathof, V. Hessel, T. Noël *Chem. Rev.* **2016**, *116*, 10276–10341.
- [8] D. Cambié, J. Dobbelaar, P. Riente, J. Vanderspikken, C. Shen, P. H. Seeberger, K. Gilmore, M. G. Debije, T. Noël *Angew. Chem. Int. Ed.* **2019**, *58*, 14374–14378; *Angew. Chem.* **2019**, *131*, 14512–14516; *Angew. Chem.* **2019**, *131*, 14512–14516.
- [9] A. Sridhar, R. Rangasamy, M. Selvaraj *New J. Chem.* **2019**, *43*, 17974–17979.
- [10] P. Li, G.-W. Wang, X. Zhu, L. Wang, *Tetrahedron* **2019**, *75*, 3448–3455.
- [11] Q.-Y. Meng, J.-J. Zhong, Q. Liu, X.-W. Gao, H.-H. Zhang, T. Lei, Z.-J. Li, K. Feng, B. Chen, C.-H. Tung, L.-Z. Wu, *J. Am. Chem. Soc.* **2013**, *135*, 19052–19055.
- [12] Z. Li, W. Zhang, Q. Zhao, H. Gu, Y. Li, G. Zhang, F. Zhang, X. Fan, *ACS Sustainable Chem. Eng.* **2015**, *3*, 468–474.
- [13] A. Dhakshinamoorthy, M. Opanasenko, J. Čejka, H. Garcia, *Catal. Sci. Technol.* **2013**, *3*, 2509.
- [14] G. Kumar, P. Solanki, M. Nazish, S. Neogi, R. I. Kureshy, N. H. Khan *J. Catal.* **2019**, *371*, 298–304.
- [15] C.-A. Wang, Y.-W. Li, X. -L.-Cheng, J.-P. Zhang, Y.-F. Han *RSC Adv.* **2017**, *7*, 408–414.
- [16] X. Yu, Z. Yang, B. Qiu, S. Guo, P. Yang, B. Yu, H. Zhang, Y. Zhao, X. Yang, B. Han, Z. Liu *Angew. Chem. Int. Ed.* **2019**, *58*, 632–636; *Angew. Chem.* **2019**, *131*, 642–646.
- [17] A. P. Schaap, A. L. Thayer, E. C. Blossey, D. C. Neckers, *J. Am. Chem. Soc.* **1975**, *97*, 13, 3741–3745.
- [18] a) For supported Eosin see review in ref [4b]; b) for other heterogeneous Eosin catalysts covalently bound to different supports see Z. Li, W. Zhang, Q. Zhao, H. Gu, Y. Li, G. Zhang, F. Zhang, X. Fan, *ACS Sustainable Chem. Eng.* **2015**, *3*, 468–47; c) for another example of column filled with glass balls and photocatalyst, see: L. Wu, D. S. Lee, H. Boufroura, M. Poliakoff, M. W. George, *ChemPhotoChem* **2018**, *2*, 580–585 and references cited.
- [19] Q. Yang, L. Zhang, C. Ye, S. Luo, L.-Z. Wu, C.-H. Tung, *Angew. Chem. Int. Ed.* **2017**, *56*, 3694–3698; *Angew. Chem.* **2017**, *129*, 3748–3752.

---

Manuscript received: April 3, 2022  
Revised manuscript received: June 23, 2022  
Accepted manuscript online: June 24, 2022  
Version of record online: July 14, 2022